Journal of Solid Mechanics Vol. 12, No. 4 (2020) pp. 969-978
DOI: 10.22034/jsm.2020.1876148.1480

Creep Life Assessment of a Super-Heater Tube

J. Jelwan *

Department of Mechanical Engineering, The Holy Spirit University of Kaslik (USEK), Jounieh, Lebanon

Received 12 August 2020; accepted 15 October 2020

ABSTRACT

Characteristics of creep deformation for 2.25Cr -1Mo were studied using the Monkman–Grant relation. A series of creep tests were conducted on 2.25Cr -1Mo at low-stress levels and at different temperatures ranging from 655 ^0C to 685^0C . The analysis of creep data indicates that 2.25Cr -1Mo is practically supported by Monkman-Grant relationship. Yet, this paper highlights the foremost difficulties associated with the parametric fitting techniques. The damage tolerance factor has been estimated to demonstrate its reliance on the loading conditions and to categorize the material strain concentration. It has been shown that at 55MPa and T=685^0C , the tertiary creep stage is not well characterized. Also, this paper identifies a need to provide a serious consideration for an appropriate creep strength factor that would be applied to pressure vessels and to improve the criteria related to design against creep and the prevention of failure.

Keywords: Creep life assessment; Remnant life; Monkman-Grant; Creep deformation mechanism; 2.25Cr -1Mo .

1 INTRODUCTION

NOWADAYS, a large amount of equipment in industry contains metallic components, which must be designed and constructed to sustain and increase their lives extended to the highest tolerable operating temperatures. The safety of these components and their economic operations will depend on how efficiently we can predict their creep lives. Therefore, most engineers are primarily concerned with the development and design of structures subjected to high temperature. There has been considerable interest in the solid state mechanics to assess the failure life from a macroscopic point of view; however, due to the difficulty of the problem especially when the components are operating at high temperature, a large amount of scatter could contaminate the extracted data. On the other hand, many mathematical models have been proposed to express the creep structural behaviour of materials using pertinent constitutive equations and a damage law [1, 2, 3]. Unfortunately, these models are valid only under certain stress and temperature conditions. Therefore, a broad-spectrum and simple method for creep life assessment of complex components without a need for non-linear analysis is desirable. Koul et al. [4] conducted an experiment on IN-738 LC blades (a nickel based super-alloy), in order to examine the validity of the Larson Miller relationship (LMP). He found out that creep stress versus the LMP scatter bands is unable to predict the service

*Corresponding author. Tel.: +961 9600906; Fax: +961 9600 970.
E-mail address: jadjelwan@usek.edu.lb (J. Jelwan).

induced in nickel based super-alloys. An unsuccessful attempt from Dyson [5] to include the CDM by generating additional restraints to the Larson Miller application were embedded. Dyson concluded [5] that LMP is sometimes inaccurate. On the other hand, Zhao et al. [6] proposed the Z-parameter method based on Larson Miller concept to assess the remaining life of steel components. They demonstrated that the value of remaining life is related to the value of probability limit. The higher value of probability limit, the lower the remaining life. Furthermore, it was shown that the normal distribution is well supported for the value of the Z parameter. Jose et al.[7], conducted an analysis for selecting adequate parameterization method for the results of creep assessment by applying the Manson Haferd [8] relationship concept and comparing it to Dorn-Sherby method [9]. Results were plotted on the Log (rupture time) versus temperature and Log (rupture time) versus inverse temperature. The analysis showed good consistency of the hot tensile results with the creep rupture data in 5 different parameterization procedures, with less scatter. Nevertheless, Manson-Haferd relationship have a consistent physical basis and doesn't present any physical meaning [7]. Satisfactory agreement is usually found for pure metals and alloys near the temperature melting point. However, care must be taking into account since some errors might be introduced especially for the activation energy evaluation where the periodic variation of the creep self-diffusion is dominant leading to a large percentage of error [7]. Likewise, Wilshire and Evans [10] clarified that the Sherby-Dorn relationship is very expensive to simulate and required lots of test programs which must be conducted to obtain the required long-term design data. On the other hand, English [11] conducted 35 creep tests at different range of temperature by applying the Dorn-Sherby correlation. He found out the confidence factor for his results were equal to 0.92. In fact, designer are interested in Dorn-Sherby parametrical creep assessment method, since it has the ability of improving the accuracy of the extrapolations. Also, it offered an excellent means of summarizing many data in a suitable form. However, deviations from linearity is normally revealed, this fact can be explained that most of the solids and metals mechanism can endure plastic deformation in different ways depending on the temperature and straining-rate circumstances [12]. Conversely, it has been shown that the Dorn-Sherby method has limited function in the temperature range [13,14]. On the other hand, a profound analytical analysis was conducted by Seruga et al.[15] to determine the time-to-rupture at low stresses and temperatures, by employing multiple methods such as Larson Miller parameter, Manson-Hafred and Sherby-Dorn relationship for comparison. Results have been compared with the R^2 value. The R^2 value confirmed that the optimum design parameters was calculated using the Mason-Hafred relationship with a 0.972 % followed by Dorn-Sherby relationship with a 0.960%. Such kind of results verifies that the Dorn-Sherby relationship offers some practical advantages with economic benefits. However, Seruga [15] didn't carry out any analysis on Monkman-Grant relationship, which has been widely used for the life time prediction. Also, Monkman-Grant relationship has a vital benefit for life time prediction which monitors the long term tests to be avoided.

Despite the fact that many researchers have extensively tested various creep parametric assessment method for the most common materials used in power plants. Yet, the methodology criteria of such assessment doesn't address a functional conformity of a large set of data in specific applications. Thus, the present paper deals with an example of application of the method procedure to the remaining life assessment of a super heater tube. The advantage of the procedure is the capability to evaluate the remaining life of a component through the execution of accelerated creep tests on service exposed material. This procedure allows for a significant reduction of the test duration without affecting the extrapolation reliability. Section 2 describes the theoretical background for predicting the life of a superheater tube operating in the creep range. Section 3 describes the application to a saturated steam nozzle and to an auxiliary steam nozzle component for which the experimental life data has been determined by testing. Section 4 discusses and summarizes the outcomes of this study. Finally, section 5 outlines the key conclusions of the investigation.

2 REMNANT LIFE FORMULATION

When dislocation motion dominate, creep strain rate for metals can be expressed by Norton Creep law which assumes that:

$$\dot{\varepsilon} = A\sigma^n \tag{1}$$

where n is the creep stress exponent and A is the solid solution strengthen defined in terms of the number fraction of transverse boundaries which are activated. Therefore, A could be represented as:

$$A = A_0 e^{\left(-\frac{Qc}{RT}\right)} \tag{2}$$

Replacing Eq. (2) into (1), the minimum creep strain rate can be rewritten in the form of an Arrhenius equation as:

$$\dot{\varepsilon}_{\min} = A_0 e^{\left(-\frac{Q_c}{RT}\right)} \sigma^n \tag{3}$$

$\dot{\varepsilon}_{\min}$ is the minimum strain rate $\left(h^{-1}\right), Q_c$ is the apparent activation energy of hot deformation $\left(J.mol^{-1}\right)$, *R* is the universal gas constant $\left(8.314 J.mol^{-1} K^{-1}\right)$, *T* is the deformation temperature (*K*). By applying the logarithmic operation on both sides to Eq. (3), the following equation is obtained:

$$ln\left(\dot{\varepsilon}_{min}\right) = ln\left(A_0\right) - Q_c / RT + n\, ln\left(\sigma\right) \tag{4}$$

The lifetime prediction can be obtained using the Monkman-Grant relationship [16]. The Monkman-Grant relationship proposed a relation between the minimum creep strain rate $\dot{\varepsilon}_{\min}$, and the rupture time t_r, as:

$$\dot{\varepsilon}_{min} . t_r^k = C_{MG} \tag{5}$$

where *k* is a constant and has a value close to unity, and it is usually expected to be between 0.65 and 1, $\dot{\varepsilon}_{min}$ is the minimum creep strain rate and C_{MG} is the Monkman-Grant constant. Eq. (5) can be approximated as:

$$t_r = \frac{C_{MG}}{\dot{\varepsilon}_{min}} = \frac{C_{MG}}{A'_0} e^{\left(\frac{Q_r}{RT}\right)} \sigma^{-m} \tag{6}$$

Comparing Eq. (3) to Eq. (6), the stress exponent *n* in Eq. (3) has been denoted as m in Eq. (6), as for the apparent activation Q_c in Eq. (3) has been denoted as Q_r in Eq. (6), because the creep stress index and the energy activation factor derived from the rupture stress temperature correlation can be different from that derived from the minimum creep rate stress temperature correlation. Eq. (6) allows to evaluate the consistency of the extracted experimental data by examining its fit within the variety of conducted tests. In fact, at a low-stress test, once the minimum creep strain rate is acquired, the time-to-rupture is sequentially estimated.

3 EXPERIMENTAL PROCEDURE

The material used in this paper was received from a steam drum which had been in service for 15 years and exposed to operation for more than 130000 *hours* at 655^0C. In order to examine the creep life prediction a tempered 2.25 *Cr* – 1 *Mo* steel pipe has been used. Creep specimens were machined from flat bars (see Fig.1), aged in the lab in an induction furnace at $600^0C \pm 2$ for 48 *hours*. All the components used in this experiment are stress relieved. Table 1 represents the chemical composition of the 2.25 Cr – 1 Mo . The design conditions for stress rupture and creep conducted in this experiment are summarized in Table 2. Using the dimensions of the steam drum and the saturated steam nozzle, and by employing the hoop stress equation $\sigma_h = PD / 2t$, the applied nominal stress has been computed. The operating pressure of the steam drum was 45.3 *MPa*, with $D_i = 230mm$ and $D_o = 350mm$. As for the auxiliary saturated steam nozzle component, the operating pressure was 20.45 MPa , with $d_i = 40mm$ and $d_o = 52mm$. Hence, the remnant life has been assessed at 39 *MPa* and 55 *MPa* for different temperature of 655^0C , 670^0C and 685^0C . Accelerated creep tests were performed according to ASTM E8M [17]. All specimens were tested in vacuum.

Table 1
Chemical Properties of the tested material (*wt*%)

C	*Si*	*Mn*	*P*	*S*	*Cr*	*Mo*	*Cu*	*N*
0.12	0.27	0.46	0.020	0.014	2.24	0.94	0.04	0.008

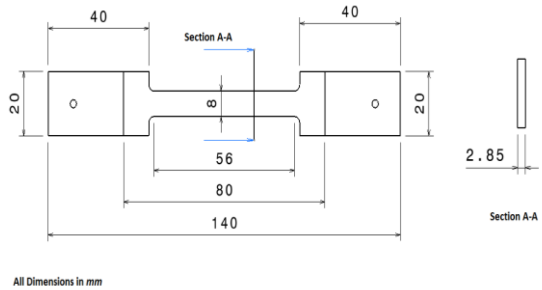

Fig.1
Creep test specimen.

Table 2
Specimen ID and design conditions.

Specimen ID	Temperature, ^0C	Stress, *MPa*
CHT1	655	39
CHT2	655	55
CHT3	670	39
CHT4	670	55
CHT5	685	39
CHT6	685	55

4 RESULTS AND DISCUSSION

Fig. 2 shows the variation of the log-log plot for the minimum creep rate $ln\left(\dot{\varepsilon}_m\right)$ versus the stress $ln\left(\sigma\right)$ at constant temperatures. A linear regression fit at a constant temperature gives n=4.82 for T=655^0C , n=5.15 for T=670^0C and n=5.52 for T=685^0C . It is clearly shown that n increases when the temperature increases. The stress exponent n is often used as an indicator for describing the dominant creep mechanism. The creep stress index n are found to be greater than 3, indicating a distinctive creep strain accumulation response of the form of conventional dislocation creep process which progresses and accelerates during the operation service conditions of any engineering power plants. At this stage, the microstructural behaviour indicates that the creep strain is governed by a continuous inter-planar slip indicating a dislocation occurrence progressed by diffusion. In fact, the deformation starts to manifest due to a slow sequence of glide assisted by an interfacial energy climb. Subsequently, creep controls the climb. Fig. 3 shows the variation of the log-log plot for the time-to-rupture $ln\left(t_r\right)$ versus the stress $ln\left(\sigma\right)$ at different temperature. This correlation incorporates the creep stress exponent m in relation to Eqs. (6). Thus, a linear regression fit gives m=-5.89 for T=655^0C , m=-4.69 for T=670^0C and m=-4.08 for T=685^0C for all measurements. The obtained results for the stress exponent m follow a diverse trend unlike the stress exponent n, where m decreases when the temperature increases. For comparison, conventional creep test results have been reported by Maruyama et al. [18] on 2.25 $Cr-1\ Mo$ steel at strain rates of $10^{-11}s^{-1}$ to $10^{-6}s^{-1}$. It has been shown that the stress exponent at high temperature takes a creep stress exponent of $n=3\sim 5$ depending on the applied stress. For convenience, Maruyama et al. [18] correlate the particle strengthened materials by stress dependence of minimum creep rates by means of a creep mechanism map for 2.25 $Cr-1\ Mo$ ranging from low stress region (*L*), intermediate-stress range to high stress region (*H*). It has been observed that the deformation characteristics is controlled by the microstructural changes and controlled by grain boundary sliding within the interaction region (*I*) indicating that the creep mechanism is mainly dominated. This observation match well with the obtained results in this paper. Fig. 4 shows the variation of the log-log plot for the minimum creep rate $ln\left(\dot{\varepsilon}_m\right)$ versus the reciprocal temperature $1/T$ at constant stresses, a linear relationship is achieved with the slope in order to obtain the creep energy activation Q_c .

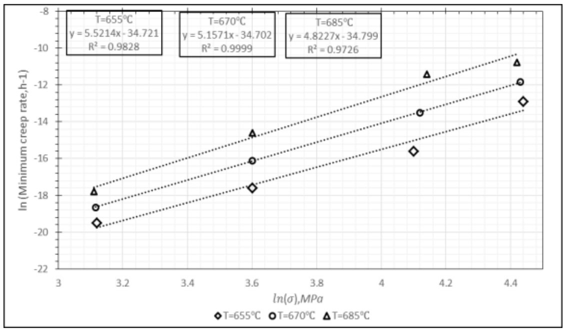

Fig.2
Variation of the minimum creep rate with respect to the applied stress at different temperature.

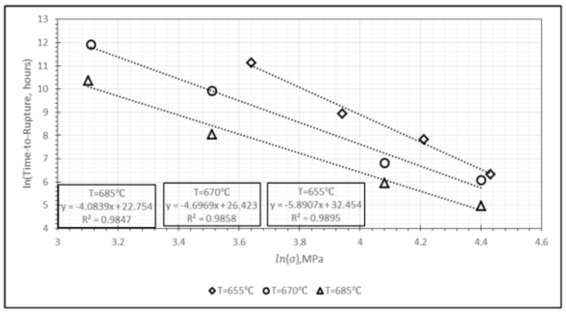

Fig.3
Stress dependence of rupture life at different temperature for 2.25*Cr*-1*Mo*.

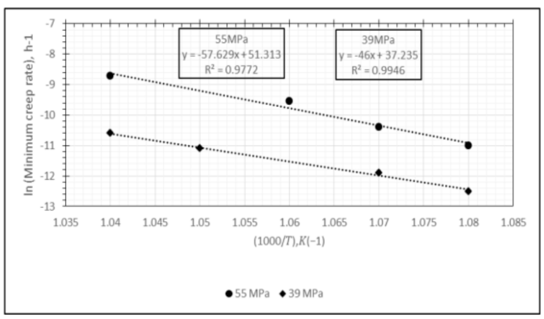

Fig.4
Temperature dependence of minimum creep rate at 39*MPa* and 55*MPa*.

Thus, a linear regression fit with an *R*-squared value equal to 0.99 gives:

$$ln\left(\dot{\varepsilon}_m\right) = -\frac{46000}{T} + 37.235 \quad \text{for} \quad \sigma = 39MPa \tag{7}$$

and

$$ln\left(\dot{\varepsilon}_m\right) = -\frac{57629}{T} + 51.313 \quad \text{for} \quad \sigma = 55MPa \tag{8}$$

Comparing Eq. (4) with Eqs. (7) and (8), Q_c is determined. For 39 *MPa*, Q_c is depicted to be equal to 382.444 *kJ/mol*, as for 55 *MPa*, Q_c is equal to 479.127 *kJ/mol* . Fig. 5 shows the variation of the log-log plot for the minimum creep rate $ln\left(\dot{\varepsilon}_m\right)$ versus the reciprocal temperature 1/*T* at constant stresses, a linear relationship is achieved with the slope in order to obtain the activation energy for creep Q_r . Thus, a linear regression fit with an *R*-squared value equal to 0.98 and 0.97 gives:

$$ln\left(t_r\right) = \frac{51153}{T} - 46.023 \quad \text{for} \quad \sigma = 39MPa \tag{9}$$

and

$$ln\left(t_r\right)=\frac{44864}{T}-41.077 \quad \text{for} \quad \sigma=55MPa \tag{10}$$

Comparing Eq. (4) with Eqs. (9) and (10), Q_r is determined. For 39 *MPa*, Q_r is depicted to be equal to 425.286 *kJ/mol* as for 55 *MPa*, $Q_r=399\,kJ/mol$. The obtained values for Q show an appropriate linear regression assessment for the creep activation energy with increasing stress for both plots, where Q_r is higher than Q_c for 39 *MPa*. This observation is inverse for 55 *MPa* where Q_r is less than Q_c . In fact, this is true since the creep activation energy Q_c is influenced by the microstructural and sub-structural changes associated with deformation, interrelated over their consequence on σ and m intuitively. Comparing this value to those obtained from the literature, it is obvious that $Q_c=364$ *kJ/mol* affirms with the work done by Parker et al. [19] who obtained $Q_c=370$ *kJ/mol* with *n*=4 , with Ray et al. [20] who obtained $Q_c=360$ *kJ/mol* with *n*=5. This variance of the results between different creep factors and constraints could arise from the dissimilarity of the microstructural inclusions among various experimentation and measurements. Moreover, under high temperature creep conditions, most of the published results are coped with limited amount of data due to the relative complexity of the problem. Thus, whenever data plots are examined for evidence from a quantitative point of view, it is more convincing to associate each measured point with a confidence limit (i.e. *R*-squared method) to follow the frequent practice. Although creep testing is biased due to its high complexity in measurements, where most of the data are contaminated by a large amount of scatter. Yet, using the R-squared tool in creep mechanics under variable consideration, primes to an intuitive and observable relation. Hence, engineers rely always to narrow or to amplify the boundaries for prediction error, where the stakes could be minor or greater. This will imply that the prediction is subjective, and it is up to the analyst to determine which corresponding values is the most favourable solution. Therefore, such procedure leads to a rather different weighting of different evidence for regular trends in creep. Considering Eqs. (4) and (7), and Eqs. (4) and (9), two A values is acquired. In this paper, the mean value is considered. Tables 3 and 4 show the measured results for the A value for different temperature and initial stress.

Table 3
Creep law coefficients and creep stress index at 39*MPa*.

Temperature	$\dot{\varepsilon}_{min}=A_0e^{\left(\frac{Q_c}{RT}\right)}\sigma^n$		$t_r=\frac{C_{MG}}{A_0'}e^{\left(\frac{Q_r}{RT}\right)}\sigma^{-m}$	
	A_0	n	A_0'	m
$655^0C\,(928.15K)$	2.4324×10^7	5.5214	2.7855×10^6	-5.8907
$670^0C\,(943.15K)$	9.240×10^7	5.1571	1.2907×10^6	-4.6969
$685^0C\,(958.15K)$	3.1457×10^8	4.48227	6.015×10^6	-4.0839

Similarly, the average A value for 55 *MPa* at different temperature is presented in Table 4.

Table 4
Creep law coefficients and creep stress index at 55 MPa.

Temperature	$\dot{\varepsilon}_{min}=A_0e^{\left(\frac{Q_c}{RT}\right)}\sigma^n$		$t_r=\frac{C_{MG}}{A_0'}e^{\left(\frac{Q_r}{RT}\right)}\sigma^{-m}$	
	A_0	n	A_0'	m
$655^0C\,(928.15K)$	4.73929×10^{12}	5.5214	7.69632×10^{11}	-5.8907
$670^0C\,(943.15K)$	2.04046×10^{13}	5.1571	2.92195×10^{11}	-4.6969
$685^0C\,(958.15K)$	7.793×10^{13}	4.48227	1.1226×10^{11}	-4.0839

Using Eq. (4), the minimum creep strain rate components in creep deformations for 55 *MPa* at *T*= 685^0C could be expressed as:

$$\dot{\varepsilon}_{min}=\left(3.90211\times10^{13}\right)\sigma^{448227}exp\left(-479.127kJ/RT\right) \tag{11}$$

Figs. 6 and 7 represent the log-log plot for the minimum creep strain rate versus the time-to-rupture subject for the 39*MPa* and 55*MPa* respectively. In order to verify the Monkman-Grant relation, a linear regression fit for 55*MPa* at $T = 685^0C$ gives:

$$\dot{\varepsilon}_{min}.t_r^{1.66} = 0.18426 \tag{12}$$

Table 5
Measured and estimated properties for 2.25*Cr-Mo* at different temperatures and pressures.

$\sigma_0\left(MPa\right)$	$T\left({}^0C\right)$	$\dot{\varepsilon}_{min}\left(h^{-1}\right)$	Time-to-minimum creep rate, (*hours*)	Time-to-rupture (*hours*)	Strain to failure	Elongation (%)
39	655	2.47E-6	371.204	5631	0.21	24.3
39	670	4.94E-5	118.84	1502	0.23	27.1
39	685	1.04E-4	107.749	1022	0.34	41.2
55	655	1.21E-4	159.23	980	0.25	29.3
55	670	2.84E-4	116.47	508	0.21	24.4
55	685	1.85E-3	63.94	98	0.19	21.1

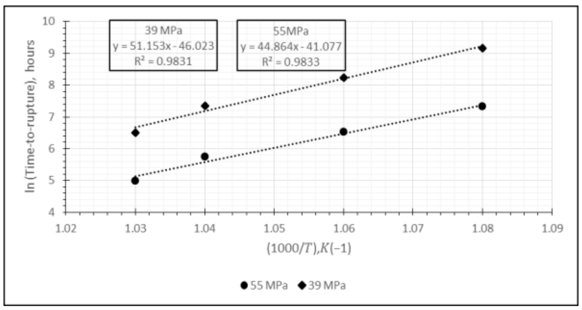

Fig.5
Temperature dependence of the time-to-rupture at 39*MPa* and 55*MPa*.

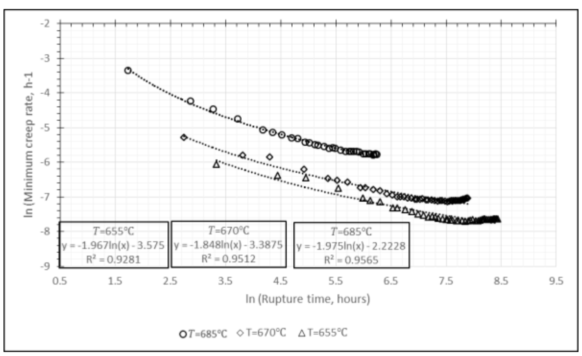

Fig.6
Variation of the rupture time with the minimum creep rate at 39 *MPa*.

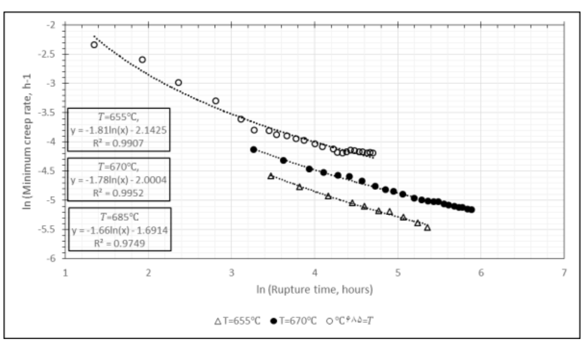

Fig.7
Variation of the rupture time with the minimum creep rate at 55 *MPa*.

Eq.(12) noticeably presents that 2.25 *Cr*-1*Mo* obeys the Monkman-Grant relation. However, comparing the exponent *k* for the Monkman-Grant Eq. (5) to many other published data [21-22], it is conspicuously shown that *k* doesn't fall within the margin of 0.65 and 1. Most of the experimental observation affirms that *k* is often between 0.65 and 1. This discrepancy could be explained by the fact that Monkman Grant constant is derived in accordance with the secondary creep stage ignoring the fact of the primary creep stage which might be a critical factor to include. Also, in this paper, the linear regression fit to the minimum strain rate has been limited between 10^{-3} s^{-1} and 10^{-9} s^{-1} , this will yield the prediction of rupture lives shorter than those obtained experimentally (please refer to Table 5 for more details). As a result, it is apparent to obtain shorter lives as it is expected. Yet, ignoring the material solid mechanics state, violates the rules of physics [1], underpinning an additional shortcoming about the Monkman Grant relation. For instance, the deficiency of any multiaxial creep stress rupture data, will prime the depiction of the creep behaviour inadequately. For example, the creep experimental assessment is primarily established on the axial net section stress, which discreetly identifies the influence of the maximum principal stress which contributes to rupture the test material. While, this distinctiveness appears to be trivial, it is of utmost importance to pinpoint it and report it in here. Also, to confirm the viability of this discussion, a simple example could be particular in relation to the ASME code VIII-Division 2 [23] which allows the use of allowable stresses S=Min(F_{avg} SR_{avg} , 0.85 R_{min}), where F_{avg} is a multiplier applied to average stress for rupture in 100,000 *hr*. At $1500^0F(815^0C)$ and below, 0.67. SR_{avg} is the average stress to cause rupture at the end of 100,000 *hours*, and SR_{min} is the minimum stress to cause rupture at the end of 100,000 *hours* [23]. In summary, the credibility of the Monkman-Grant relationship with the very similar value of k is depreciated either by the dissimilarity in the tested materials properties and their microstates, i.e. the use of different technique for heat treatment or in their homologous behaviour for different temperatures. Practically, the tertiary creep stage is evident during the secondary creep stage and it is associated by cavities affecting the acceleration of the creep strain rate accumulation. Consequently, void growth progresses till it reach an acute value where the tertiary creep stage is significantly observed. This perception is correlated to the continuum creep damage mechanics (CDM) tolerance factor which has been extensively discussed in [24]. Hence, damage is treated as an internal state variable that assesses the susceptibility of a material to localized cracking at strain concentrations [22]. It is suggested to be a better measure of creep ductility as it is related to the ability of a material to redistribute stresses [22]. λ is defined as the ratio of strain to rupture to MGD as:

$$\lambda = \frac{\varepsilon_r}{\left(\dot{\varepsilon}_{min}.t_r\right)} \tag{13}$$

From Eq.(13) the product $\dot{\varepsilon}_{min}.t_r$ represents the ductility of the material within the secondary creep stage. Hence, comparing Eq. (5) to Eq. (13) the product $\dot{\varepsilon}_{min}.t_r$ could be replaced by the Monkman Grant constant such as $C_{MG} \approx \dot{\varepsilon}_{min}.t_r$. Moreover, the failure strain ε_r could be represented by the total elongation (δ) of the material during the creeping process. Therefore, the damage tolerance factor could be modified and represented as:

$$\lambda = \frac{\delta}{C} \tag{14}$$

Using the predicted and measured values from Table 5, the characteristic performance of the material is computed and reported in Table 6.

Table 6
Evaluation of the damage tolerance factor.

$\sigma_0(MPa)$	$T\left({}^0C\right)$	DAMAGE TOLERANCE FACTOR (λ) – EQ. (14)
39	655	8.67
39	670	8.01
39	685	3.80
55	655	2.49
55	670	1.8
55	685	1.14

From Table 6, it is clearly shown that the material exhibits high λ for the 39*MPa*, whereas it is low for 55 *MPa*. The failure mechanism with high damage tolerance factor indicates that the material fails due to substructure softening damage mechanism with low strain concentration [22]. On the other hand, low damage tolerance factor indicates that failure occurs due to growth of cavities coupled by diffusion and power law creep by reducing the net section area causing damage to the material [22]. It should be noted, at 55 *MPa* and at T=685 , the damage tolerance factor is $1.14 \prec 1.5$ indicating that the tertiary creep stage is not well characterized.

5 CONCLUSION

The lifetime of a superheater tube made from 2.25 *Cr*-1*Mo* is tested experimentally. Monkman-Grant relation was employed to evaluate the consistency of the mined experimental data by probing its fit within the scatter multitude for all tests. Once a minimum creep rate has been determined in a low-stress test, rupture life can be estimated without running the test to failure. Although Monkman and Grant stated that this relationship was not intended for extrapolation [16], many application has been applied for that purpose [25-27], particularly when only low-stress tests are acceptable to prevent large initial plastic strains. However, the Monkman-Grant equation is not capable to emphasize the disintegration effects caused during service [27]. In fact, this aspect is related to the complex experimental data issues, which are normally contaminated by the scatter obtained from multifaceted alloys [1]. Finally, this paper identifies a need to provide a serious consideration for an appropriate creep strength factor which would be applied to pressure vessels and to improve the criteria related to design against creep and the prevention of failure.

REFERENCES

[1] Jelwan J., Chowdhury M., Pearce G., 2013, Design for creep: a critical examination of some methods, *Engineering Failure Analysis* **27**: 350-372.

[2] Jelwan J., Chowdhury M., Pearce G., 2011, Creep life design criterion and its applications to pressure vessel codes, *Materials Physics and Mechanics* **11**: 157-182.

[3] Zarrabi K., Jelwan J., 2010, A mesoscopic damage model for predicting the plastic-creep life of welded joints subjected to quasi-static loading, *Proceedings of ASME IMECE, ASME 2010 International Mechanical Engineering Congress & Exposition*, Vancouver, British Columbia, Canada.

[4] Koul A.K., Castillo R., Willett K., 1984, Creep life predictions in nickel-based superalloys, *Materials Science and Engineering* **66**(2): 213-226.

[5] Dyson B., 2000, Use of CDM in materials modeling and component creep life prediction, *Journal of Pressure Vessel Technology* **122**(3): 281-296.

[6] Zhao J., Li D.-M., Fang Y.-Y., 2010, Application of manson-haferd and larson-miller methods in creep rupture property evaluation of heat-resistant steels, *Journal of Pressure Vessel Technology* **132**(6): 064502.

[7] José F., Sobrinhoand dos R., Levi de O.B., 2005, Correlation between creep and hot tensile behaviour for2.25*Cr*-1*Mo* steel from 500^0C to 700^0C, *An Assessment According to Different Parameterization Methodologies, Revista Matérial* **10**(3): 463-471.

[8] Manson S.S., Haferd A.M., 1953, A linear time-temperature relation for extrapolation of creep and stress-rupture data, *NASA-TN-2890*.

[9] Dorn J.E., 1955, Some fundamental experiments on high temperature creep, *Journal of the Mechanics and Physics of Solids* **3**(2): 85-88.

[10] Wilshire B., Evans R.W., 1994, Acquisition and analysis of creep data, *The Journal of Strain Analysis for Engineering Design* **29**(3): 159-165.

[11] English R.E., 1991, *9th Symposium on Space Nuclear Power Systems*, Albuqerque.

[12] Brozzo P., 1963, A method for the extrapolation of creep and stress-rupture data of complex alloys, Proceedings of the Institution of Mechanical Engineers **178**(31): 77-85.

[13] Woo G.K., Nam S.Y., Woo S. R., 2005, Application and standard error analysis of the parametric methods for predicting the creep life of type 316LN SS, *Key Engineering Materials* **297-300**: 2272-2277.

[14] Larke E.C., Inglis N.P., 1963, A critical examination of some methods of analysing and extrapolating stress-rupture data, *Proceedings of the Institution of Mechanical Engineers* **178**(31): 33-47.

[15] Seruga D., Nagode M., 2011, Unification of the most commonly used time-temperature creep parameters, *Materials Science and Engineering: A* **528**(6): 2804-2811.

[16] Monkman F.C. , Grant N.J. , 1956, Lifetime prediction under constant load creep conditions for a cast ni-base superalloy*, Proceedings ASTM* **56**: 593.

[17] ASTM E8 / E8M-13, 2013, *Standard Test Methods for Tension Testing of Metallic Materials*, ASTM International, West Conshohocken.

[18] Maruyama K., Sawada K., Koike J., Sato H., Yagi K., 1997, Examination of deformation mechanism maps in 2.25*Cr*—1*Mo* steel by creep tests at strain rates of 10−11 to 10−6 *s*−1, *Materials Science and Engineering: A* **224**(1–2): 166-172.

[19] Parker J.D., Parsons A.W.J., 1995, High temperature deformation and fracture processes in 214Cr1Mo-12Cr12Mo14V weldments, *International Journal of Pressure Vessels and Piping* **63**(1): 45-54.

[20] Ray A.K., Tiwari Y.N., Roy P.K., Chaudhuri S., Bose S.C., Ghosh R.N., Whittenberger J.D., 2007, Creep rupture analysis and remaining life assessment of 2.25*Cr*–1*Mo* steel tubes from a thermal power plant, *Materials Science and Engineering: A* **454–455**: 679-684.

[21] Bueno Levi de O., Vitor Luiz S., Marino L., 2005, Constant load creep data in air and vacuum on 2.25*Cr*-1*Mo* steel from 600 °*C* to 700 °*C*, *Materials Research* **8**(4): 401-408.
[22] Choudhary B.K., Isaac Samuel E., 2011, Creep behaviour of modified 9*Cr*–1*Mo* ferritic steel, *Journal of Nuclear Materials* **412**(1): 82-89.
[23] ASME Boiler and Pressure Vessel Code, Section VIII, Division 1 and Section III, Division 1, Subsection NH, Class I Components in Elevated Temperatures Service, 2001.
[24] Jelwan J. 2017, Prediction of creep rupture in 2.25*Cr*–1*Mo* notched bars, *Journal of Applied Mechanics and Technical Physics* **58**(1): 129-138.
[25] Dimmler G., Weinert P., Cerjak H., 2008, Extrapolation of short-term creep rupture data--The potential risk of over-estimation, *International Journal of Pressure Vessels and Piping* **85**(1-2): 55-62.
[26] Evans M., 1999, Further analysis of the Monkman-Grant relationship for 2.25*Cr*-1*Mo* steel using creep data from the national research institute for metals, *Advances in Physical Metallurgy* **15**(1): 91-100.
[27] Nickel H., Ennis P.J., Quadakkers W.J., 2001, The creep rupture properties of 9% chromium steels and the influence of oxidation on strength, *Mineral Processing and Extractive Metallurgy Review: An International Journal* **22**(1): 181 - 195.